Optimized BD-ZF Precoder for Multiuser MIMO-VFDM Cognitive Transmission

Rugui Yao, Juan Xu, Geng Li, and Ling Wang

In this paper, we study an optimized block-diagonal zero-forcing (BD-ZF) precoder in a two-tiered cognitive network consisting of a macro cell (MC) and a small cell (SC). By exploiting multiuser multiple-input and multiple-output Vandermonde-subspace frequency-division multiplexing (VFDM) transmission, a cognitive SC can coexist with an MC. We first devise a cross-tier precoder based on the idea of VFDM to cancel the interference from the SC to the MC. Then, we propose an optimized BD-ZF intra-tier precoder (ITP) to suppress multiuser interference and maximize the throughput in the SC. In the case where the dimension of a provided null space is larger than that required by the BD-ZF ITP, the optimized BD-ZF ITP can collect all limited channel gain by optimizing rotating and selecting matrices. Otherwise, the optimized BD-ZF ITP is validated to be equivalent to the conventional BD-ZF ITP in terms of throughput. Numerical results are presented to demonstrate the throughput improvement of the proposed optimized BD-ZF ITP and to discover the impact of imperfect channel state information.

Keywords: Capacity, precoder, cognitive transmission, determinant maximization, BD-ZF, VFDM.

I. Introduction

With the increasing demand on high-speed wireless communications, more spectrum resources are required. Techniques such as cognitive radio (CR) [1] and heterogeneous networks [2] have been recently proposed to improve spectrum efficiency.

In two-tiered networks, small cells (SCs) coexist with a macro cell (MC) in an overlay manner. The SCs and the MC share a common spectrum; the MC has precedence over this spectrum. By sharing the common spectrum, the capacity for the whole network can be significantly improved.

In a two-tiered cognitive network, the main challenge is how to manage the cross-interference from the SCs to the MC. To achieve the highest possible spectral efficiency, the MC and the SCs usually work in complete sharing mode [3]. In this mode, interference management techniques, such as dirty paper coding [4], opportunistic interference alignment [5], [6], and spectrum shaping [7], must be used to protect an MC transmission from interference or reduce the interference to within a tolerable range.

Vandermonde-subspace frequency-division multiplexing (VFDM) has been recently proposed to enable a two-tiered network to work in complete sharing mode [3], [8]–[13]. It exploits the available degrees of freedom (DoF) left over by the cyclic prefix (CP) removal in an MC orthogonal frequency-division multiplexing (OFDM) transmission. By adopting a cross-tier precoder (CTP) to project the transmitted signal of an SC onto the null space of a channel from the SC to the MC, VFDM can prevent an SC transmission from generating interference to the MC; therefore, spectrum reuse can be achieved. Actually, VFDM can be regarded as interference alignment (IA) realization within the frequency domain [12]

Manuscript received Jan. 31, 2015; revised Nov. 1, 2015; accepted Nov. 11, 2015.

This work has been supported in part by the National Natural Science Foundation of China (No. 61501376), the Natural Science Basic Research Plan in Shaanxi Province of China (No. 2014JM2-6094), and the State Key Laboratory of Rail Traffic Control and Safety (No. RCS2015ZQ004).

Rugui Yao (corresponding author, yaorg@nwpu.edu.cn), Geng Li (785462603@qq.com), and Ling Wang (lingwang@nwpu.edu.cn) are with the School of Electronics and Information, Northwestern Polytechnical University, Xi'an, China.

Juan Xu (xuj@mail.nwpu.edu.cn) is with the School of Electronic and Control Engineering, Chang'an University, Xi'an, China.

rather than in the spatial domain [5], [14], [15].

In [3], [8], and [9], VFDM transmission is considered in a simplified two-tiered network comprising one MC and one SC, where a CTP can be constructed by a Vandermonde matrix. For an orthogonal frequency-division multiple access (OFDMA)–based multiuser MC, a subspace-based precoder is proposed in [3], [11], and [16] as an extension of a single-user MC.

A multiuser VFDM with multiple SCs is introduced in [10] and [11], where each SC consists of a transmitter and a receiver. A block-diagonalized CTP is devised independently at the transmitter of each SC, without requiring information from any of the other transmitters.

A multiuser cooperative CTP scheme is proposed in [17], where the DoF of the cognitive network improves significantly. Exploiting the improved DoF, a block-diagonal zero-forcing (BD-ZF) intra-tier precoder (ITP) with simple structure is also developed in [17] to handle the interference among SCs. However, when the dimension of the null space for the BD-ZF ITP design is large, [17] does not consider an optimized design for the BD-ZF ITP they develop. With the increased DoF [17], a capacity-achieving (CA) ITP is proposed in [18] to improve the throughput of SCs, but with high complexity. In [13] and [19], the study of VFDM is extended to MIMO systems.

In this paper, we consider a multiple-input and multiple-output Vandermonde-subspace frequency-division multiplexing (MIMO-VFDM) cognitive network comprising an MC and an SC, where the SC's transmitter is equipped with multiple antennas. In the case where the dimension of the provided null space is larger than that required by the BD-ZF ITP, an optimized BD-ZF ITP is developed to collect all channel gain. As a result, the throughput is improved significantly. Numerical results are also presented to demonstrate the effectiveness of the optimized BD-ZF ITP.

The rest of this paper is organized as follows. The system model of a two-tiered cognitive network is described in Section II. The CTP based on VFDM is derived in Section III. In Section IV, the transmitted dimension of a conventional BD-ZF ITP is analyzed and an optimized BD-ZF ITP is then developed. Numerical results are presented in Section V. Finally, a conclusion is given in Section VI.

II. System Model

The two-tiered cognitive network considered in this paper comprises a Long-Term Evolution OFMDA-based MC and a MIMO-VFDM-based SC, as shown in Fig. 1. The MC in the first tier includes an MC base station (MBS) and an MC user (MU), while the SC in the second tier is composed of an SC base station (SBS) and N_{SU} SC users (SUs). Both the MC and the SC share a common frequency band, but it is the MC that has the priority to access the spectrum. In the system of Fig. 1, we consider the MBS, MU, and SUs to all be equipped with only one antenna, whereas the SBS is considered to be equipped with N_T antennas.

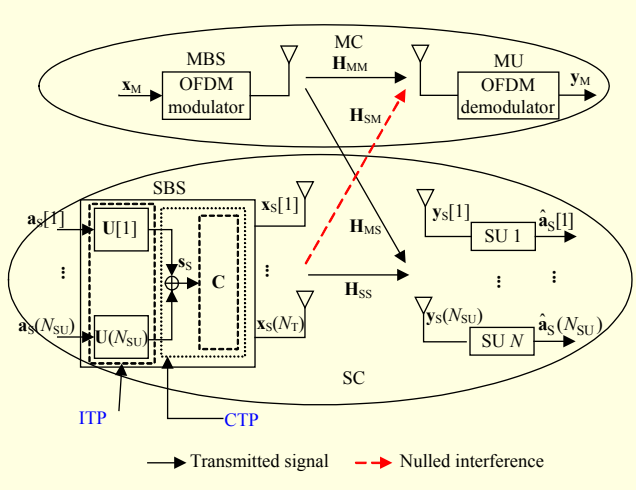

Fig. 1. Coexistence of OFDMA-based MC and MIMO-VFDM-based SC.

In this paper, we consider only the downlink transmission of both the MC and the SC. For coexistence, a CTP is adopted to cancel the interference from the SC to the MC, and an optimized BD-ZF ITP is developed to suppress the interference among the SUs. Note that we consider only one MU in the MC. However, all results can be easily extended to the case of multiple MUs [3], [11], [16].

In the MC, an OFDM transmission with block size K and CP length L is adopted. The received signal vector, $\mathbf{y}_M \in \mathcal{C}^{K\times 1}$, at the MU can be denoted as

$$\mathbf{y}_M = \mathbf{H}_{MM}\mathbf{x}_M + \mathbf{H}_{SM}\mathbf{x}_S + \mathbf{n}_M, \quad (1)$$

where $\mathbf{H}_{MM} \in \mathcal{C}^{K\times K}$ denotes the frequency response matrix of the channel from the MBS to the MU; $\mathbf{x}_M \in \mathcal{C}^{K\times 1}$ is the transmitted symbol vector from the MBS; $\mathbf{H}_{SM} \in \mathcal{C}^{K\times N_T(K+L)}$ represents the overall cross-tier channel matrix from the SBS to the MU; $\mathbf{x}_S \in \mathcal{C}^{N_T(K+L)\times 1}$ indicates the transmitted symbol vector from the SBS; and $\mathbf{n}_M \in \mathcal{C}^{K\times 1}$ denotes $\mathcal{CN}(\mathbf{0}, \sigma_M^2\mathbf{I}_K)$ distributed additive noise with variance σ_M^2. Further, $\mathbf{x}_S$ is precoded by both the CTP and the optimized BD-ZF ITP, whose designs will be discussed later.

In a time-invariant channel, when the CP of the OFDM is long enough, $\mathbf{H}_{MM}$ is diagonal and can be represented $\mathbf{H}_{MM} = \mathrm{diag}\{H_0, H_1, \ldots, H_{K-1}\}$ [3], where H_k denotes the frequency response of the kth subcarrier.

The second term in (1) represents the cross-tier interference from the SBS to the MU. The overall cross-tier channel matrix

can be denoted as

$$\mathbf{H}_{\mathrm{SM}} = \left(\mathbf{H}_{\mathrm{SM}}[1], \mathbf{H}_{\mathrm{SM}}[2], \ldots, \mathbf{H}_{\mathrm{SM}}[N_{\mathrm{T}}]\right), \quad (2)$$

where $\mathbf{H}_{\mathrm{SM}}[n] \in \mathcal{C}^{K\times(K+L)}$ is the interference channel matrix from the nth antenna at the SBS to the MU; $\mathbf{H}_{\mathrm{SM}}[n]$ can be formulated as

$$\mathbf{H}_{\mathrm{SM}}[n] = \mathbf{F}\boldsymbol{\Gamma}_{\mathrm{SM}}[n], \quad (3)$$

where $\mathbf{F} = \left\{\frac{1}{\sqrt{K}} e^{-\mathrm{j}\frac{2\pi(k-1)(l-1)}{K}}\right\}_{k,l=1}^{K} \in \mathcal{C}^{K\times K}$ is a discrete Fourier transform matrix and $\boldsymbol{\Gamma}_{\mathrm{SM}}[n] \in \mathcal{C}^{K\times(K+L)}$ is a Toeplitz time-domain channel matrix [3], [11], [20], [21]. We denote $\{\mathbf{h}_{\mathrm{SM}}[n,l]\}_{l=0}^{L}$ as the time-domain channel impulse response (CIR) from the nth antenna at the SBS to the MU, and $\boldsymbol{\Gamma}_{\mathrm{SM}}[n]$ can be defined as

$$\boldsymbol{\Gamma}_{\mathrm{SM}}[n] = \begin{pmatrix} \mathbf{h}_{\mathrm{SM}}[n,L] & \cdots & \mathbf{h}_{\mathrm{SM}}[n,0] & 0 & 0 \\ \vdots & \ddots & & \ddots & \vdots \\ 0 & 0 & \mathbf{h}_{\mathrm{SM}}[n,L] & \cdots & \mathbf{h}_{\mathrm{SM}}[n,0] \end{pmatrix}. \quad (4)$$

We denote $\mathbf{x}_{\mathrm{S}}[n] \in \mathcal{C}^{(K+L)\times 1}$ for $n = 1, 2, \ldots, N_{\mathrm{T}}$ as the transmitted signal vector at the nth antenna at the SC. The overall transmitted symbol vector, $\mathbf{x}_{\mathrm{S}}$, at the SBS can be represented as

$$\mathbf{x}_{\mathrm{S}} = \begin{pmatrix} \mathbf{x}_{\mathrm{S}}[1] \\ \vdots \\ \mathbf{x}_{\mathrm{S}}[N_{\mathrm{T}}] \end{pmatrix}. \quad (5)$$

In the SC, the overall received signal vector, $\mathbf{y}_{\mathrm{S}} \in \mathcal{C}^{N_{\mathrm{SU}}K\times 1}$, at N_{SU} SUs can be expressed as

$$\mathbf{y}_{\mathrm{S}} = \mathbf{H}_{\mathrm{SS}}\mathbf{x}_{\mathrm{S}} + \mathbf{H}_{\mathrm{MS}}\mathbf{x}_{\mathrm{M}} + \mathbf{n}_{\mathrm{S}}, \quad (6)$$

where $\mathbf{H}_{\mathrm{MS}}\mathbf{x}_{\mathrm{M}} \in \mathcal{C}^{N_{\mathrm{SU}}K\times 1}$ and $\mathbf{n}_{\mathrm{S}} \in \mathcal{C}^{N_{\mathrm{SU}}K\times 1}$ represent the interference from the MC and $\mathcal{CN}(\mathbf{0}, \sigma_{\mathrm{S}}^2\mathbf{I}_{N_{\mathrm{SU}}K})$-distributed additive noise with variance σ_{S}^2, respectively; and $\mathbf{H}_{\mathrm{SS}} \in \mathcal{C}^{N_{\mathrm{SU}}K\times N_{\mathrm{T}}(K+L)}$ denotes the overall channel matrix from the SBS to all SUs within the SC.

We define $\mathbf{y}_{\mathrm{S}}[m] \in \mathcal{C}^{K\times 1}$ as the received signal vector at the mth SU; then, $\mathbf{y}_{\mathrm{S}}$ can be represented as

$$\mathbf{y}_{\mathrm{S}} = \begin{pmatrix} \mathbf{y}_{\mathrm{S}}[1] \\ \vdots \\ \mathbf{y}_{\mathrm{S}}[N_{\mathrm{SU}}] \end{pmatrix}. \quad (7)$$

The channel matrix, $\mathbf{H}_{\mathrm{SS}}$, can be represented as

$$\mathbf{H}_{\mathrm{SS}} = \begin{pmatrix} \mathbf{F}\boldsymbol{\Gamma}_{\mathrm{SS}}[1,1] & \cdots & \mathbf{F}\boldsymbol{\Gamma}_{\mathrm{SS}}[N_{\mathrm{T}},1] \\ \vdots & & \vdots \\ \mathbf{F}\boldsymbol{\Gamma}_{\mathrm{SS}}[1,N_{\mathrm{SU}}] & \cdots & \mathbf{F}\boldsymbol{\Gamma}_{\mathrm{SS}}[N_{\mathrm{T}},N_{\mathrm{SU}}] \end{pmatrix}, \quad (8)$$

where $\boldsymbol{\Gamma}_{\mathrm{SS}}[n,m]$ (for $n = 1, \ldots, N_{\mathrm{T}}$, $m = 1, \ldots, N_{\mathrm{SU}}$) denotes the Toeplitz time-domain channel matrix from the nth antenna at the SBS to the mth SU.

As $\mathbf{H}_{\mathrm{SM}}[n]$ in (3), the overall interference channel matrix, $\mathbf{H}_{\mathrm{MS}} \in \mathcal{C}^{N_{\mathrm{SU}}K\times K}$, from the MBS to all SUs can be formulated as

$$\mathbf{H}_{\mathrm{MS}} = \begin{pmatrix} \mathbf{H}_{\mathrm{MS}}[1] \\ \vdots \\ \mathbf{H}_{\mathrm{MS}}[N_{\mathrm{SU}}] \end{pmatrix}, \quad (9)$$

where $\mathbf{H}_{\mathrm{MS}}[m] = \mathbf{F}\boldsymbol{\Gamma}_{\mathrm{MS}}[m]\mathbf{A}\mathbf{F}^{-1} \in \mathcal{C}^{K\times K}$ for $m = 1, \ldots, N_{\mathrm{SU}}$ denotes the interference channel matrix from the MBS to the mth SU, which is diagonal due to OFDM transmission. Here, the Toeplitz time-domain channel matrix, $\boldsymbol{\Gamma}_{\mathrm{MS}}[m]$, can be constructed from $\{\mathbf{h}_{\mathrm{MS}}[n,l]\}_{l=0}^{L}$ as (4), and the CP insertion matrix is given by $\mathbf{A} = \begin{pmatrix} \mathbf{0}_{L\times(K-L)} & \mathbf{I}_L \\ & \mathbf{I}_K \end{pmatrix}$.

Note that, from (1), the SBS requires a perfect cross-tier channel matrix, $\mathbf{H}_{\mathrm{SM}}$, to design a precoder that can guarantee an interference-free transmission in the MC.

In time-division duplexing communications, channels can be estimated by using the reciprocity of uplink and downlink channels, while channel state information (CSI) can be exchanged over the backhaul between the MBS and the SBS in frequency-division duplexing communications. Both the procedure and overhead for the acquisition of CSI are significant challenges in a two-tiered cooperative network and beyond the concern of this paper.

III. CTP for Cognitive Network

To guarantee an interference-free transmission in the MC, a CTP is adopted at the SBS to preprocess any interference, as the second term in (1), to be 0; that is,

$$\mathbf{H}_{\mathrm{SM}}\mathbf{x}_{\mathrm{S}} = \mathbf{0}. \quad (10)$$

We denote $\mathbf{C} \in \mathcal{C}^{N_{\mathrm{T}}(K+L)\times J}$ to be the CTP and $\mathbf{s}_{\mathrm{S}} \in \mathcal{C}^{J\times 1}$ to be the transmitted signal vector prior to precoding by the CTP, where J is the overall transmitted dimension of the SBS; that is, the number of symbols that the SBS can transmit simultaneously. The overall transmitted dimension, J, will be discussed later. With the CTP, the transmitted signal vector at the SBS, $\mathbf{x}_{\mathrm{S}}$, can be expressed as

$$\mathbf{x}_{\mathrm{S}} = \mathbf{C}\mathbf{s}_{\mathrm{S}}. \quad (11)$$

Substituting (11) into (10), we can conclude the condition for the interference-free transmission in the MC is as follows:

$$\mathbf{H}_{\mathrm{SM}}\mathbf{C} = \mathbf{0}. \quad (12)$$

If the SBS can acquire CSI, $\mathbf{H}_{SM}$, then a CTP, $\mathbf{C}$, can be devised from (12) to completely cancel out the interference from the SBS to the MU. From (12), $\mathbf{C}$ is located in the null space of $\mathbf{H}_{SM}$.

Using singular value decomposition (SVD), the interference channel matrix, $\mathbf{H}_{SM}$, can be rewritten as

$$\mathbf{H}_{SM} = \mathbf{U}_{CTP}\mathbf{\Lambda}_{CTP}\mathbf{V}_{CTP}^{H}, \tag{13}$$

where $\mathbf{U}_{CTP} \in \mathcal{C}^{K\times K}$ and $\mathbf{V}_{CTP} \in \mathcal{C}^{N_T(K+L)\times N_T(K+L)}$ are both unitary and $\mathbf{\Lambda}_{CTP} \in \mathcal{C}^{K\times N_T(K+L)}$ is diagonal. The rectangle matrix, $\mathbf{\Lambda}_{CTP}$, can be divided as follows:

$$\mathbf{\Lambda}_{CTP} = (\mathbf{\Sigma}_{CTP}, \mathbf{0}_{K\times[(N_T-1)K+N_TL]}), \tag{14}$$

where $\mathbf{\Sigma}_{CTP} \in \mathcal{C}^{K\times K}$ is a diagonal matrix whose diagonal elements are composed of the singular values of $\mathbf{H}_{SM}$. Further, we define $\mathbf{V}_1 \in \mathcal{C}^{N_T(K+L)\times K}$ and $\mathbf{V}_2 \in \mathcal{C}^{N_T(K+L)\times[(N_T-1)K+N_TL]}$ as the submatrices of $\mathbf{V}_{CTP}$ to satisfy ($\mathbf{V}_1$, $\mathbf{V}_2$). Then, we have

$$\mathbf{H}_{SM} = \mathbf{U}_{CTP}\mathbf{\Lambda}_{CTP}(\mathbf{V}_1, \mathbf{V}_2)^{H} = \mathbf{U}_{CTP}\mathbf{\Sigma}_{CTP}\mathbf{V}_1^{H}. \tag{15}$$

From (15), $\mathbf{H}_{SM}\mathbf{V}_2 = \mathbf{U}_{CTP}\mathbf{\Sigma}_{CTP}\mathbf{V}_1^{H}\mathbf{V}_2 = \mathbf{0}$ due to the orthogonality that exists between $\mathbf{V}_1$ and $\mathbf{V}_2$. Therefore, considering the condition for the interference-free transmission in (12), the CTP can be defined as

$$\mathbf{C} = \mathbf{V}_2 \in \mathcal{C}^{N_T(K+L)\times[(N_T-1)K+N_TL]}. \tag{16}$$

As $\mathbf{C} = \mathbf{V}_2 \in \mathcal{C}^{N_T(K+L)\times[(N_T-1)K+N_TL]}$ in (16), we have $J = (N_T-1)K + N_TL$. In the above derivation, we assume that $\mathbf{\Sigma}_{CTP}$ is with full row rank; otherwise, the dimension of the CTP will increase, resulting in more symbols being transmitted at the SBS. In the subsequent discussion, $\mathbf{\Sigma}_{CTP}$ is assumed to be full row ranked.

IV. BD-ZF ITP

In the SC, the ITP is also required to suppress the interference among the SUs. Due to its simple structure and good performance, BD-ZF is usually used to construct an ITP. In this section, we focus on BD-ZF ITP design and present an analysis on the available transmitted dimension for each SU. To maximize the capacity in the SC, an optimized BD-ZF ITP is then developed.

1. Principle for BD-ZF ITP

Considering the CTP $\mathbf{C}$ in Section III, we can rewrite the received signals at the SUs in (6) as

$$\mathbf{y}_S = \mathbf{H}_{SS}\mathbf{C}\mathbf{s}_S + \mathbf{w}_S = \bar{\mathbf{H}}_{SS}\mathbf{s}_S + \mathbf{w}_S, \tag{17}$$

where $\bar{\mathbf{H}}_{SS} = \mathbf{H}_{SS}\mathbf{C} \in \mathcal{C}^{N_{SU}K\times[(N_T-1)K+N_TL]}$ and $\mathbf{w}_S = \mathbf{H}_{MS}\mathbf{x}_M + \mathbf{n}_S \in \mathcal{C}^{N_{SU}K\times 1}$, which consists of the interference $\mathbf{H}_{MS}\mathbf{x}_M$ and noise $\mathbf{n}_S$. From (17), when $N_{SU}K \le [(N_T-1)K + N_TL]$, BD-ZF can be adopted to suppress the interference among the SUs [22].

Further, we define $\mathbf{U}[m] \in \mathcal{C}^{[(N_T-1)K+N_TL]\times D[m]}$ and $\mathbf{a}[m] \in \mathcal{C}^{D[m]\times 1}$ as the BD-ZF ITP and the transmitted symbols for the mth SU, respectively, where $D[m]$ is the dimension of $\mathbf{a}[m]$. The transmitted signal of the SBS can finally be represented as

$$\mathbf{s}_S = \sum_{m=1}^{N_{SU}} \mathbf{U}[m]\mathbf{a}[m]. \tag{18}$$

Substituting (18) into (17), we have

$$\mathbf{y}_S = \bar{\mathbf{H}}_{SS}\sum_{m=1}^{N_{SU}} \mathbf{U}[m]\mathbf{a}[m] + \mathbf{w}_S. \tag{19}$$

From (19), we can separate the received signal at the mth SU as

$$\begin{aligned}\mathbf{y}_S[m] &= \bar{\mathbf{H}}_{SS}[m]\mathbf{U}[m]\mathbf{a}[m] \\ &\quad + \sum_{i=1, i\neq m}^{N_{SU}} \bar{\mathbf{H}}_{SS}[m]\mathbf{U}[i]\mathbf{a}[i] + \mathbf{w}_S[m],\end{aligned} \tag{20}$$

where $\bar{\mathbf{H}}_{SS}[m] \in \mathcal{C}^{K\times[(N_T-1)K+N_TL]}$ and $\mathbf{w}_S[m] \in \mathcal{C}^{K\times 1}$ are constructed from the $[(m-1)K+1]$ th row to the mKth row of $\bar{\mathbf{H}}_{SS}$ and $\mathbf{w}_S$, respectively. We denote $\mathbf{R}_{\mathbf{w}}[m] = \mathrm{E}(\mathbf{w}_S[m]\mathbf{w}_S^{H}[m])$ as the covariance of $\mathbf{w}_S[m]$, which is diagonal for diagonal characteristics of $\mathbf{H}_{MS}[m]$ in an OFDM transmission.

According to the principle of BD-ZF, the BD-ZF ITP for the mth SU, $\mathbf{U}[m]$, needs to be located within the null space of the following matrix:

$$\begin{aligned}\mathcal{H}_{SS}^{(m)} &= \big(\bar{\mathbf{H}}_{SS}^{H}[1], \ldots, \bar{\mathbf{H}}_{SS}^{H}[m-1], \bar{\mathbf{H}}_{SS}^{H}[m+1], \ldots, \\ &\quad \bar{\mathbf{H}}_{SS}^{H}[N_{SU}]\big)^{H} \in \mathcal{C}^{[(N_{SU}-1)K]\times[(N_T-1)K+N_TL]}.\end{aligned} \tag{21}$$

From (21), $\mathcal{H}_{SS}^{(m)}$ has a null space of at least dimension $N_{null}[m] = N_TL + (N_T - N_{SU})K$. We denote $\mathbf{V}_{null}[m] \in \mathcal{C}^{[(N_T-1)K+N_TL]\times N_{null}[m]}$ as an orthonormal basis in the null space of $\mathcal{H}_{SS}^{(m)}$ for simplification. We still utilize an SVD to find $\mathbf{V}_{null}[m]$. We take the SVD of $\mathcal{H}_{SS}^{(m)}$ as

$$\mathcal{H}_{SS}^{(m)} = \mathbf{U}_{SS}[m]\mathbf{\Lambda}_{SS}[m]\mathbf{V}_{SS}^{H}[m], \tag{22}$$

where $\mathbf{U}_{SS}[m] \in \mathcal{C}^{(N_{SU}-1)K\times(N_{SU}-1)K}$ and $\mathbf{V}_{SS}[m] \in \mathcal{C}^{[(N_T-1)K+N_TL]\times[(N_T-1)K+N_TL]}$ are unitary and $\mathbf{\Lambda}_{SS}[m] \in \mathcal{C}^{[(N_{SU}-1)K]\times[(N_T-1)K+N_TL]}$ is diagonal. As a result, we can construct $\mathbf{V}_{null}[m]$ with the last $N_{null}[m]$ columns of $\mathbf{V}_{SS}[m]$; that is,

$$\mathbf{V}_{null}[m] = \mathbf{V}_{SS}[m]\big(:, (N_{SU}-1)K+1 : (N_T-1)K+N_TL\big). \tag{23}$$

From the derivation above, we can conclude that the BD-ZF ITP, $\mathbf{U}[m]$, is located in the space spanned by $\mathbf{V}_{\text{null}}[m]$. In the following subsection, we will construct $\mathbf{U}[m]$ with $\mathbf{V}_{\text{null}}[m]$.

2. Transmitted Dimension Analysis

For $\mathbf{V}_{\text{null}}[m] \in \mathcal{C}^{[(N_{\text{T}}-1)K+N_{\text{T}}L]\times N_{\text{null}}[m]}$ and $\mathbf{U}[m] \in \mathcal{C}^{[(N_{\text{T}}-1)K+N_{\text{T}}L]\times D[m]}$, the transmitted dimension of the mth SU, $D[m]$, satisfies

$$D[m] \le N_{\text{null}}[m]. \tag{24}$$

From (17), the overall transmitted dimension in the SC is $(N_{\text{T}}-1)K + N_{\text{T}}L$; thus, we have

$$\sum_{m=1}^{N_{\text{SU}}} D[m] \le (N_{\text{T}}-1)K + N_{\text{T}}L. \tag{25}$$

As in a MIMO transmission [23], the solvable dimension is less than the minimum of the overall transmitted and received dimension of the transmission in (20); so, $D[m]$ has the constraint

$$D[m] \le \min\{(N_{\text{T}}-1)K + N_{\text{T}}L, K\}. \tag{26}$$

Combining (24), (25), and (26), we can achieve the following relationship:

$$\begin{cases} N_{\text{SU}} N_{\text{null}}[m] \le \left[(N_{\text{T}}-1)K + N_{\text{T}}L\right] \le N_{\text{SU}}K \\ \quad \text{if} \quad 1 \le N_{\text{T}} \le \left((N_{\text{SU}}+1)K\right)/(K+L), \\ N_{\text{SU}}K < \left[(N_{\text{T}}-1)K + N_{\text{T}}L\right] < N_{\text{SU}} N_{\text{null}}[m] \\ \quad \text{if} \quad N_{\text{T}} > \left((N_{\text{SU}}+1)K\right)/(K+L). \end{cases} \tag{27}$$

From (27), the maximal transmitted dimension of the mth SU, $D[m]$, will be

$$\begin{cases} D[m] \le N_{\text{null}}[m] & 1 \le N_{\text{T}} \le \left((N_{\text{SU}}+1)K\right)/(K+L), \\ D[m] \le K & N_{\text{T}} > \left((N_{\text{SU}}+1)K\right)/(K+L). \end{cases} \tag{28}$$

Figures 2 and 3 illustrate the available transmitted dimension achieved by the BD-ZF ITP (see shaded areas). In Fig. 2, we assume that N_{SU} is fixed and consider how $D[m]$ changes with an increase of N_{T}. From Fig. 2, as long as $N_{\text{null}}[m] > K$ (that is, $N_{\text{T}} > (N_{\text{SU}}+1)K/(K+L)$), the dimension of the provided null space will be larger than the dimension required by the BD-ZF ITP. In this case, we should devise an optimized strategy to construct a BD-ZF ITP from large dimension. In Fig. 3, N_{T} is supposed to be fixed and the impact of the number of SUs is considered. In the case of $N_{\text{SU}} \le (N_{\text{T}}(K+L)/K - 1)$, the same optimized strategy is required to design a BD-ZF ITP. With an increase of N_{SU}, $D[m]$ is decreased to be 0 when $N_{\text{SU}} > N_{\text{T}}(K+L)/K$. From Fig. 3, we discover the interesting phenomenon that the number of SUs, N_{SU}, can be larger than the number of transmitted antennas at the SBS, N_{T} (for example, $N_{\text{SU}} = (N_{\text{T}}(K+L)/K - 1) \ge N_{\text{T}}$ when $N_{\text{T}} \ge K/L$). This is attributed to the frequency-domain DoF provided by VFDM.

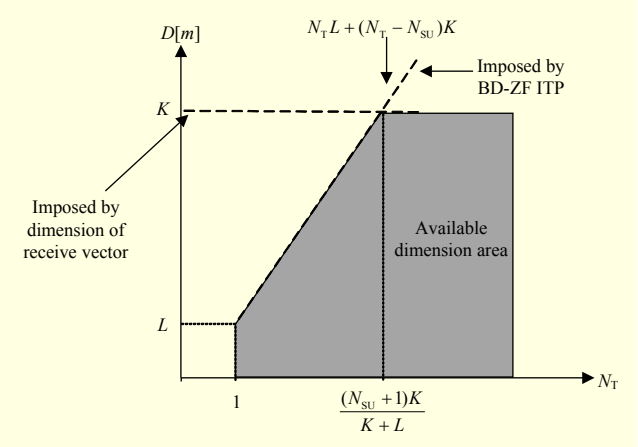

Fig. 2. Relationship between available transmitted dimension of BD-ZF ITP and N_{T}.

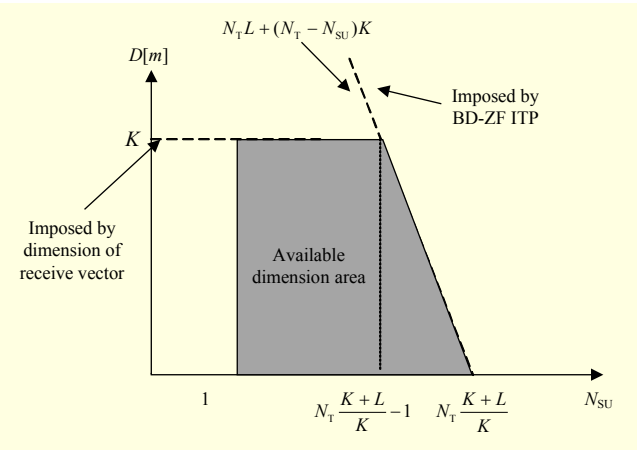

Fig. 3. Relationship between available transmitted dimension of BD-ZF ITP and N_{SU}.

3. Optimized BD-ZF ITP Design

In this section, we optimize the BD-ZF ITP in terms of capacity maximization. From Fig. 2, when $1 \le N_{\text{T}} \le (N_{\text{SU}}+1)K/(K+L)$, the BD-ZF ITP, $\mathbf{U}[m]$, and $\mathbf{V}_{\text{null}}[m]$ have the same dimension. In this case, we should find a rotating matrix, $\mathbf{T}[m] \in \mathcal{C}^{N_{\text{null}}[m]\times D[m]}$ onto $\mathbf{V}_{\text{null}}[m]$ to maximize the capacity of the mth SU. When $N_{\text{T}} > (N_{\text{SU}}+1)K/(K+L)$, $\mathbf{V}_{\text{null}}[m]$ has a larger dimension than $\mathbf{U}[m]$. Thus, we should devise a rotating and selecting matrix, $\mathbf{T}[m] \in \mathcal{C}^{N_{\text{null}}[m]\times D[m]}$ onto $\mathbf{V}_{\text{null}}[m]$ to achieve capacity maximization. Considering the two cases above, we formulate the optimized BD-ZF ITP as

$$\mathbf{U}[m] = \mathbf{V}_{\text{null}}[m]\mathbf{T}[m], \tag{29}$$

where all columns of $\mathbf{T}[m]$ are required to be orthonormal without changing the transmitted power for each SU and generating any interference among SUs. Note that to maximize the capacity of the mth SU, we set the transmitted dimension, $D[m]$, to be $N_{\text{null}}[m]$ when $1 \le N_{\text{T}} \le (N_{\text{SU}}+1)K/(K+L)$ and K when $N_{\text{T}} > (N_{\text{SU}}+1)K/(K+L)$.

With the BD-ZF ITP, the interference among the SUs is completely suppressed. Substituting (29) into (20), the received signal at the mth SU is represented as

$$\mathbf{y}_{\text{S}}[m] = \bar{\mathbf{H}}_{\text{SS}}[m]\mathbf{V}_{\text{null}}[m]\mathbf{T}[m]\mathbf{a}[m] + \mathbf{w}_{\text{S}}[m]. \tag{30}$$

In (30), the interference from the MC still exists. To maximize capacity, a whitening filter at the mth SU, $\mathbf{Q}[m] = \mathbf{R}_{\mathbf{w}}^{-1/2}[m]$, is adopted to whiten the interference-plus-noise.

With the analysis above, the capacity of the channel from the SBS to the mth SU can be represented as

$$\begin{aligned} C[m] = \frac{1}{K+L}\log_2 \Big| \mathbf{I}_K + \mathbf{Q}[m]\bar{\mathbf{H}}_{\text{SS}}[m]\mathbf{V}_{\text{null}}[m] \\ \times \mathbf{T}[m]\mathbf{P}[m]\mathbf{T}^{\text{H}}[m]\mathbf{V}_{\text{null}}^{\text{H}}[m]\bar{\mathbf{H}}_{\text{SS}}^{\text{H}}[m]\mathbf{Q}^{\text{H}}[m] \Big|, \end{aligned} \tag{31}$$

where $\mathbf{P}[m] = \text{E}\left(\mathbf{a}[m]\mathbf{a}^{\text{H}}[m]\right) = \text{diag}\left(P_1^m, \ldots, P_{D[m]}^m\right)$ denotes the power allocation matrix for the transmission of the mth SU. For fairness, the total power, P_{S}, is equally allocated to each SU; that is, $P_{\text{S}}/N_{\text{SU}} \ge \sum_{i=1}^{D[m]} P_i^m$. Considering the power constraint, the solution of $\mathbf{T}[m]$ can be formulated as an optimization problem, as follows:

$$\begin{aligned} \max_{\mathbf{T}[m],\mathbf{P}[m]} \quad & C[m] \\ \text{s.t.} \quad & \text{Trace}\left(\mathbf{P}[m]\right) \le P_{\text{S}}/N_{\text{SU}}. \end{aligned} \tag{32}$$

Due to the monotone characteristics of $f(x) = \log_2(x)$, only the determinant in (31) is considered. For simplification of representation, let $\mathbf{X}[m] = \mathbf{Q}[m]\bar{\mathbf{H}}_{\text{SS}}[m]\mathbf{V}_{\text{null}}[m] \in \mathcal{C}^{K \times N_{\text{null}}[m]}$ and $\mathbf{Y}[m] = \mathbf{T}[m]\mathbf{P}[m]\mathbf{T}^{\text{H}}[m] \in \mathcal{C}^{N_{\text{null}}[m] \times N_{\text{null}}[m]}$. We rewrite the determinant in the object function in (32) as

$$\begin{aligned} & \Big| \mathbf{I}_K + \mathbf{Q}[m]\bar{\mathbf{H}}_{\text{SS}}[m]\mathbf{V}_{\text{null}}[m]\mathbf{T}[m]\mathbf{P}[m] \\ & \quad \times \mathbf{T}^{\text{H}}[m]\mathbf{V}_{\text{null}}^{\text{H}}[m]\bar{\mathbf{H}}_{\text{SS}}^{\text{H}}[m]\mathbf{Q}^{\text{H}}[m] \Big| \\ & = \left| \mathbf{I}_K + \mathbf{X}[m]\mathbf{Y}[m]\mathbf{X}^{\text{H}}[m] \right| \\ & = \left| \mathbf{I}_{N_{\text{null}}[m]} + \mathbf{X}^{\text{H}}[m]\mathbf{X}[m]\mathbf{Y}[m] \right|, \end{aligned} \tag{33}$$

where the derivation of the second equation utilizes Sylvester's determinant theorem $\left|\mathbf{I}_p + \mathbf{\Phi\Psi}\right| = \left|\mathbf{I}_q + \mathbf{\Psi\Phi}\right|$ when $\mathbf{\Phi} \in \mathcal{C}^{p \times q}$ and $\mathbf{\Psi} \in \mathcal{C}^{q \times p}$ [24].

Applying Gram–Schmidt orthogonalization, we can extend $\mathbf{T}[m]$ to a complete orthonormal basis, $\tilde{\mathbf{T}}[m] \in \mathcal{C}^{N_{\text{null}}[m] \times N_{\text{null}}[m]}$, such as $\tilde{\mathbf{T}}[m] = (\mathbf{T}[m],\ \mathbf{T}_{\text{ex}}[m])$ where $\mathbf{T}_{\text{ex}}[m] \in \mathcal{C}^{N_{\text{null}}[m] \times (N_{\text{null}}[m] - D[m])}$. We can then extend $\mathbf{P}[m]$ to a diagonal matrix with more dimensions, as in

$$\tilde{\mathbf{P}}[m] = \text{diag}\left(P_1^m, P_2^m, \ldots, P_{D[m]}^m, \underbrace{0, \ldots, 0}_{N_{\text{null}}[m] - D[m]} \right). \tag{34}$$

Consequently, the Hermitian matrix $\mathbf{Y}[m]$ can be diagonalized as

$$\mathbf{Y}[m] = \tilde{\mathbf{T}}[m]\tilde{\mathbf{P}}[m]\tilde{\mathbf{T}}^{\text{H}}[m]. \tag{35}$$

Meanwhile, the Hermitian matrix $\mathbf{X}^{\text{H}}[m]\mathbf{X}[m]$ can also be diagonalized using eigenvalue decomposition (EVD) as

$$\mathbf{X}^{\text{H}}[m]\mathbf{X}[m] = \mathbf{Q}_{\text{xx}}[m]\mathbf{\Lambda}_{\text{xx}}[m]\mathbf{Q}_{\text{xx}}^{\text{H}}[m], \tag{36}$$

where $\mathbf{Q}_{\text{xx}}[m] \in \mathcal{C}^{N_{\text{null}}[m] \times N_{\text{null}}[m]}$ is unitary and $\mathbf{\Lambda}_{\text{xx}}[m]$ is diagonal, consisting of the eigenvalues of $\mathbf{X}^{\text{H}}[m]\mathbf{X}[m]$.

According to Lemma 3 in [25], to maximize the determinant, $\left|\mathbf{I}_{N_{\text{null}}[m]} + \mathbf{X}^{\text{H}}[m]\mathbf{X}[m]\mathbf{Y}[m]\right|$ in (33), $\mathbf{Y}[m]$ and $\mathbf{X}^{\text{H}}[m]\mathbf{X}[m]$ must be simultaneously diagonalized. Considering (35) and (36), simultaneous diagonalization of $\mathbf{Y}[m]$ and $\mathbf{X}^{\text{H}}[m]\mathbf{X}[m]$ must give rise to $\tilde{\mathbf{T}}[m] = \mathbf{Q}_{\text{xx}}[m]$; thus, we have

$$\mathbf{T}[m] = \mathbf{Q}_{\text{xx}}[m]\left(:, 1 : D[m]\right). \tag{37}$$

Combining (33), (35), (36) and $\tilde{\mathbf{T}}[m] = \mathbf{Q}_{\text{xx}}[m]$, the capacity in (31) can be rewritten as

$$\begin{aligned} C[m] &= \frac{1}{K+L}\log_2 \Big| \mathbf{I}_{N_{\text{null}}[m]} + \mathbf{Q}_{\text{xx}}[m]\mathbf{\Lambda}_{\text{xx}}[m]\mathbf{Q}_{\text{xx}}^{\text{H}}[m] \\ &\qquad \times \mathbf{Q}_{\text{xx}}[m]\tilde{\mathbf{P}}[m]\mathbf{Q}_{\text{xx}}^{\text{H}}[m] \Big| \\ &= \frac{1}{K+L}\log_2 \left| \mathbf{I}_{N_{\text{null}}[m]} + \mathbf{\Lambda}_{\text{xx}}[m]\tilde{\mathbf{P}}[m] \right|. \end{aligned} \tag{38}$$

Referring to (28), we have $D[m] = \text{rank}(\mathbf{Y}[m]) \le \text{rank}(\mathbf{X}^{\text{H}}[m]\mathbf{X}[m])$. Then, (38) can be represented as

$$C[m] = \frac{1}{K+L}\sum_{i=1}^{D[m]} \log_2 \left| 1 + \mathbf{\Lambda}_{\text{xx}}[m,i]P_i^m \right|, \tag{39}$$

where $\mathbf{\Lambda}_{\text{xx}}[m,i]$ denotes the ith diagonal entry of $\mathbf{\Lambda}_{\text{xx}}[m]$. Since $\mathbf{X}[m]$ has no relationship with $\mathbf{T}[m]$ and $\mathbf{P}[m]$, $\mathbf{\Lambda}_{\text{xx}}[m]$ can be obtained directly from (36). When the power constraint in (32) and the object function in (39) are considered, a water-filling power allocation algorithm [26] can be applied to calculate $\mathbf{P}[m]$ and maximize the capacity of the mth SU.

For the other SUs, we can take the same process to devise their own optimized BD-ZF ITPs and maximize their capacities.

V. Numerical Results

In this section, we present numerical results to demonstrate the effectiveness of the proposed optimized BD-ZF ITP. The system setting for simulations is listed as follows. An OFDM transmission adopted by the MC has a bandwidth of 1.92 MHz with $K = 64$ and $L = 16$. All CIRs are assumed to be time-invariant complex Gaussian distributed random variables; that is, $\mathbf{h}_{\mathrm{SM}}[n], \mathbf{h}_{\mathrm{SS}}[n,m], \mathbf{h}_{\mathrm{MS}}[m] \sim \mathcal{CN}(\mathbf{0}, \mathbf{I}_{L+1}/(L+1))$ [3], [11]. Unless specified otherwise, we always assume the power allocated to the MC and the SC to be P_{m} and P_{S}, respectively, which is always equal to one; that is, we have $P_{\mathrm{m}} = P_{\mathrm{S}} = 1$. For comparison, we present the capacities for the non-optimized BD-ZF ITPs constructed with the first $D[m]$ columns or the $D[m]$ randomly selected columns from the basis $\mathbf{V}_{\mathrm{null}}[m]$ in (23). We mark these two schemes as "direct" and "random," respectively, while marking the proposed scheme "optimal" in the following figures.

1. Perfect CSI

In this subsection, perfect CSI is always assumed to be available for the MBS/MU or the SBS/SUs if they require CSI. The capacity of the SC is evaluated for different SNRs, different numbers of SUs, different numbers of antennas, and different amounts of interference from the MC.

Figure 4 shows the sum capacity of the SC for different numbers of SUs with $N_{\mathrm{T}} = 8$ when SNR =10 dB and 30 dB. In general, the optimized BD-ZF ITP outperforms the non-optimized ones in terms of sum capacity. However, when $N_{\mathrm{T}}(K+L)/K - 1 \le N_{\mathrm{SU}} \le N_{\mathrm{T}}(K+L)/K$, such as $N_{\mathrm{SU}} = 9$, all the ITPs achieve the same throughput. In the Appendix, we prove $\mathbf{T}[m]$ has no impact on throughput in this case. From Fig. 4, we also observe that, even if $N_{\mathrm{SU}} = 9 > N_{\mathrm{T}}$, that is, the number of SUs is larger than the number of transmitted antennas at the SBS, the SC can still fulfill transmission. This realization results from the utilization of the frequency-domain DoF provided by VFDM. Moreover, there is an optimal number of SUs, $N_{\mathrm{SU}}^{\mathrm{opt}}$, for all the ITPs, when considering the relationship between sum capacity and N_{SU}. When the number of SUs increases from 1 to $N_{\mathrm{SU}}^{\mathrm{opt}}$, the throughput increases due to the involvement of more users. However, when N_{SU} continues to increase from $N_{\mathrm{SU}}^{\mathrm{opt}}$ to 9, the throughput decreases, because the reduced power allocated for the transmission of each SU becomes the dominant factor. In this and the following figures, we can observe that the two non-optimized BD-ZF ITPs obtain almost the same capacity.

Figure 5 compares the capacity of the optimized and non-optimized BD-ZF ITPs versus N_{T}, with $N_{\mathrm{SU}} = 2$ for SNR = 10 dB and 30 dB, respectively. As we can see, the optimized and non-optimized BD-ZF ITPs have the same throughput when $N_{\mathrm{T}} = 2$. This is attributed to the same reason as the case of $N_{\mathrm{SU}} = 9$ in Fig. 4. We can refer to the Appendix to account for the result in the case of $N_{\mathrm{T}} < (N_{\mathrm{SU}}+1)K/(K+L)$. The optimized BD-ZF ITP obviously outperforms the non-optimized ones. The optimized BD-ZF ITP increases monotonically as the number of transmitted antennas at the SBS increases, whereas the non-optimized ITPs do not share such a trend. From Fig. 2, we can find that, for the non-optimized BD-ZF ITPs, the available transmitted dimension of each SU increases when N_{T} increases from two to three, which results in an increasing sum capacity. On the contrary, when N_{T} increases from three onwards, the sum capacity decreases.

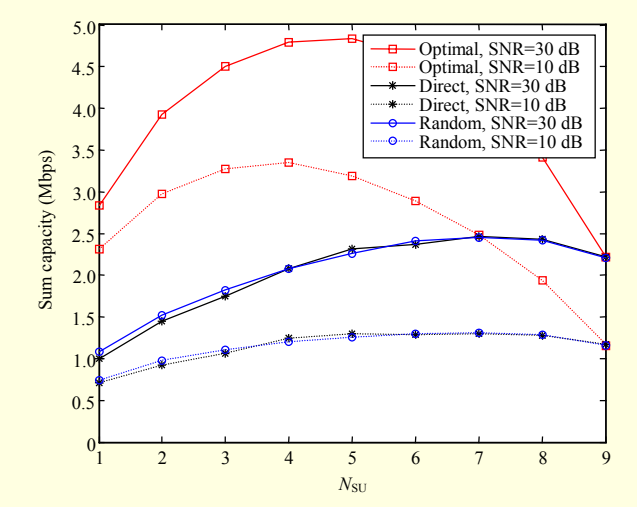

Fig. 4. Sum capacity vs. number of SUs, N_{SU}, for $N_{\mathrm{T}} = 8$.

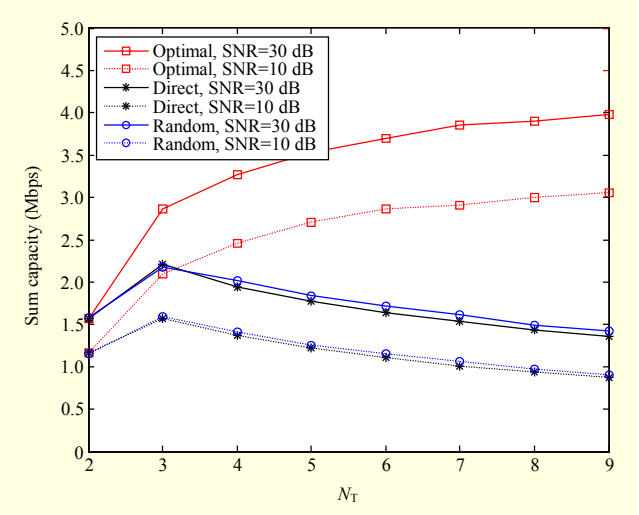

Fig. 5. Sum capacity vs. number of antennas, N_{T}, for $N_{\mathrm{SU}} = 2$.

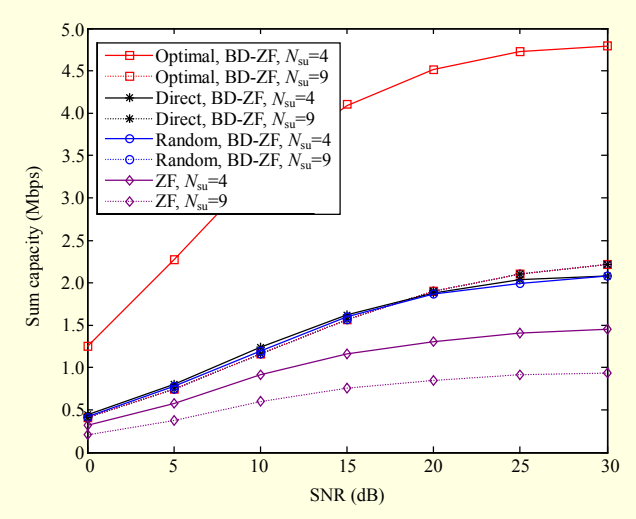

Fig. 6. Sum capacity at different SNRs for $N_T = 8$.

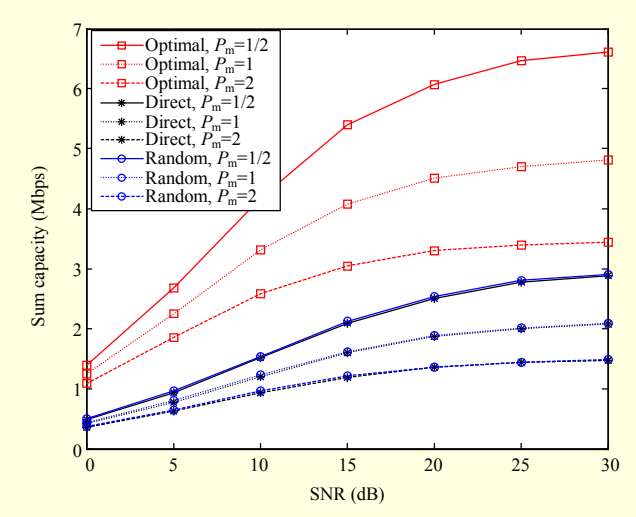

Fig. 7. Sum capacity at different SNRs with different power allocated to MC for $N_T = 8$, $N_{SU} = 4$, and $P_S = 1$.

When $N_T \geq 3$, the transmitted dimension stays at $D[m] = K$, while the dimension of the null space, $\mathbf{V}_{null}[m] \in \mathcal{C}^{[(N_T-1)K+N_TL]\times N_{null}[m]}$, increases given that $N_{null}[m] = (N_T-1)K + N_TL$. With the increase of N_T, the limited channel gain of $\mathbf{H}_{SS}[m] \in \mathcal{C}^{K\times N_T(K+L)}$ spreads all over the enlarging space of the equivalent channel matrix, $\mathbf{H}_{SS}[m]\mathbf{CV}_{null}[m] \in \mathcal{C}^{K\times[(N_T-1)K+N_TL]}$. If we select the first, or random, $D[m]$ columns from $\mathbf{V}_{null}[m]$ to construct the non-optimized BD-ZF ITPs, then only partial channel gain of $\mathbf{H}_{SS}[m]\mathbf{CV}_{null}[m]$ will be collected. As a result, the achievable throughput for the non-optimized BD-ZF ITPs decreases when N_T increases from three onwards. By comparison, our optimized BD-ZF ITP can always collect all channel gain to achieve good performance of sum capacity.

Figure 6 compares the sum capacity of the optimized and non-optimized BD-ZF ITPs at different SNRs for $N_T = 8$. In the case of $N_{SU} = 4$, the optimized BD-ZF ITP outperforms the non-optimized ones, which demonstrates the capacity improvement of our optimized BD-ZF ITP. However, when $N_{SU} = 9$, all BD-ZF ITPs achieve the same performance. We can refer to Fig. 4 and the Appendix for an account. In Fig. 6, the capacity of a ZF ITP [27] is also presented. Although the ZF ITP can simplify the receiver structure, it requires a higher power budget to achieve the same throughput as BD-ZF ITP (conventional or optimized) due to its severe power normalization factor for satisfying the constraint of maximum transmitted power at each transmitter [27]. The ZF ITP, therefore, obtains a lower capacity than the BD-ZF ITPs in the cases of $N_{SU} = 4$ and $N_{SU} = 9$.

Figure 7 compares the sum capacity of the optimized and non-optimized BD-ZF ITPs at different SNRs with different power allocated to the MC for $N_T = 8$, $N_{SU} = 4$, and $P_S = 1$. When the power allocated to the MC is increased, the SC suffers from more severe interference from the MC (see $\mathbf{H}_{MS}\mathbf{x}_M$ in (6)), thus obtaining a lower throughput. However, due to the utilization of the CTP, the MC performs interference-free transmission and has the same capacity regardless of the power allocated to the SC.

2. Imperfect CSI

In the previous designs of both the CTP and the BD-ZF ITP, perfect CSI was always assumed to be available. However, in a practical implementation, channel estimation techniques can only yield imperfect CSI. Given this, we adopt the channel estimation in [10] to evaluate the impact of imperfect CSI on the throughput of the two-tiered network. As in [10], the training duration, τ, is assigned for the channel estimation. For simplicity, an infinite-capacity backhaul is assumed to be available and the overhead of CSI exchange is therefore ignored. This allows us to focus on the analysis of the impact of channel estimation error. The study of the achievable throughput under limited backhaul capacity will be an interesting subject of our future work.

Figure 8 shows the impact of imperfect CSI on the sum capacities of both the MC and the SC for $N_T = 8$, $N_{SU} = 4$, and $\tau = 10K$ (10 OFDM symbols). We can observe the prominent degradation of the throughput for the two systems. For the OFDMA-based transmission of the MC, imperfect CSI brings out inter-subcarrier interference. Besides this, the design of a CTP with imperfect CSI cannot thoroughly cancel out the interference from the SC to the MC. These two factors attribute to the performance loss of the MC. The sum capacity of the SC is also decreased evidently due to the imperfect CSI. With

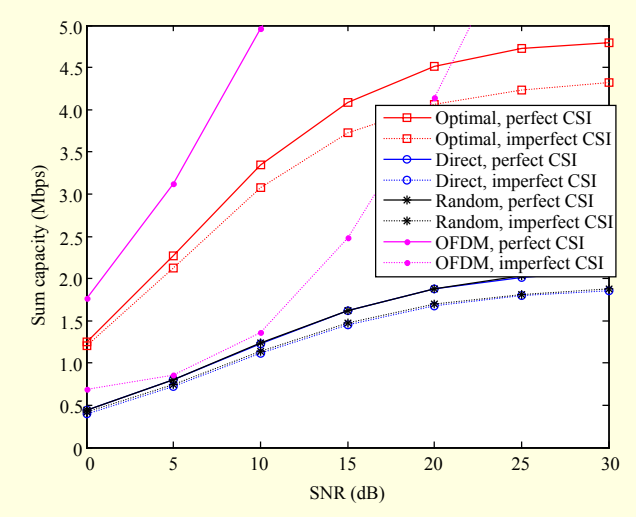

Fig. 8. Sum capacities of MC and SC with imperfect CSI for $N_T = 8$, $N_{SU} = 4$, and $\tau = 10K$.

imperfect CSI, the interference from the MC and noise cannot be whitened well; since the interference among the SUs cannot be suppressed completely, multiuser interference emerges.

VI. Conclusion

In this paper, we have proposed an optimized BD-ZF ITP design for multiuser MIMO-VFDM cognitive downlink transmission. We have first analyzed the relationship between transmitted dimension and the number of SUs and transmitted antennas at an SBS. When constructing the BD-ZF ITP, in the case where the dimension of the provided null space is larger than that required by the BD-ZF ITP, we have derived the BD-ZF ITP by optimizing the rotating and selecting matrix in terms of sum capacity. Numerical results have demonstrated the optimized BD-ZF ITP can collect all channel gain and thus achieve good performance of sum capacity. Furthermore, we have investigated the impact of imperfect CSI introduced by practical channel estimation. The proposed precoder can be used to improve the capacity of a cognitive system.

Appendix

From the analysis in Section IV-2, when $N_{SU} \geq N_T(K+L)/K - 1$ or $N_T \leq (N_{SU}+1)K/(K+L)$, the available transmitted dimension for the mth SU, $D[m]$, is equal to the dimension of the provided null space spanned by $\mathbf{V}_{null}[m]$; that is, $D[m] = N_{null}[m]$. For optimized BD-ZF ITP, from (34), (37), and (38), we have

$$\mathbf{T}[m] = \mathbf{Q}_{xx}[m], \tag{40}$$

$$C[m] = \frac{1}{K+L}\log_2 \left| \mathbf{I}_{N_{null}[m]} + \mathbf{\Lambda}_{xx}[m]\mathbf{P}[m] \right|. \tag{41}$$

When the non-optimized BD-ZF ITPs are adopted, the first, or the random, $D[m]$ columns of $\mathbf{V}_{null}[m]$ are selected to construct BD-ZF ITP. Note that when $N_{SU} \geq N_T(K+L)/K - 1$ or $N_T \leq (N_{SU}+1)K/(K+L)$, $D[m] = N_{null}[m]$. Therefore, $\mathbf{T}[m] \in \mathcal{C}^{N_{null}[m] \times D[m]}$ can be rewritten as

$$\mathbf{T}[m] = \mathbf{I}_{N_{null}[m]}. \tag{42}$$

Substituting (36) and (42) into (31), we have

$$C[m] = \frac{1}{K+L}\log_2 \left| \mathbf{I}_{N_{null}[m]} + \mathbf{Q}_{xx}[m]\mathbf{\Lambda}_{xx}[m]\mathbf{Q}_{xx}^{H}[m]\mathbf{P}[m] \right|. \tag{43}$$

Regarding the unitary characteristics of $\mathbf{Q}_{xx}[m]$ and Sylvester's determinant theorem [24], (43) becomes

$$C[m] = \frac{1}{K+L}\log_2 \left| \mathbf{I}_{N_{null}[m]} + \mathbf{\Lambda}_{xx}[m]\mathbf{P}[m] \right|. \tag{44}$$

Comparing (41) and (44), we conclude that the optimized and non-optimized BD-ZF ITPs achieve the same throughput when $N_{SU} \geq N_T(K+L)/K - 1$ or $N_T \leq (N_{SU}+1)K/(K+L)$.

References

[1] X. Hong et al., "Cognitive Radio Networks," *IEEE Veh. Technol. Mag.*, vol. 4, no. 4, Dec. 2009, pp. 76–84.

[2] A. Damnjanovic et al., "A Survey on 3GPP Heterogeneous Networks," *IEEE Wireless Commun.*, vol. 18, no. 3, June 2011, pp. 10–21.

[3] L.S. Cardoso et al., "Vandermonde-Subspace Frequency Division Multiplexing for Two-Tiered Cognitive Radio Networks," *IEEE Trans. Commun.*, vol. 61, no. 6, June 2013, pp. 2212–2220.

[4] N. Devroye, P. Mitran, and V. Tarokh, "Achievable Rates in Cognitive Radio Channels," *IEEE Trans. Inf. Theory*, vol. 52, no. 5, May 2006, pp. 1813–1827.

[5] S.M. Perlaza et al., "From Spectrum Pooling to Space Pooling: Opportunistic Interference Alignment in MIMO Cognitive Networks," *IEEE Trans. Signal Process.*, vol. 58, no. 7, July 2010, pp. 3728–3741.

[6] S.M. Perlaza et al., "Opportunistic Interference Alignment in MIMO Interference Channels," *IEEE Int. Symp. Pers., Indoor Mobile Radio Commun.*, Cannes, France, Sept. 15–18, 2008, pp. 1–5.

[7] W. Zhang and U. Mitra, "Spectrum Shaping: A New Perspective on Cognitive Radio-Part I: Coexistence with Coded Legacy Transmission," *IEEE Trans. Commun.*, vol. 58, no. 6, June 2010, pp. 1857–1867.

[8] L.S. Cardoso et al., "Vandermonde Frequency Division Multiplexing

for Cognitive Radio," *IEEE Workshop Signal Process. Adv. Wireless Commun.*, Recife, Brazil, July 6–9, 2008, pp. 421–425.

[9] L.S. Cardoso et al., "Vandermonde-Subspace Frequency Division Multiplexing Receiver Analysis," *IEEE Int. Symp. Pers. Indoor Mobile Radio Commun.*, Istanbul, Turkey, Sept. 26–30, 2010, pp. 293–298.

[10] M. Maso et al., "Channel Estimation Impact for LTE Small Cells Based on MU-VFDM," *IEEE Wireless Commun. Netw. Conf.*, Shanghai, China, Apr. 1–4, 2012, pp. 2560–2565.

[11] M. Maso et al., "Cognitive Orthogonal Precoder for Two-Tiered Networks Deployment," *IEEE J. Sel. Areas Commun.*, vol. 31, no. 11, Nov. 2013, pp. 2338–2348.

[12] L. Lu et al., "Opportunistic Transmission Exploiting Frequency- and Spatial-Domain Degrees of Freedom," *IEEE Wireless Commun.*, vol. 21, no. 2, Apr. 2014, pp. 91–97.

[13] L. Lu, G. Li, and A. Maaref, "Spatial-Frequency Signal Alignment for Opportunistic Transmission," *IEEE Trans. Signal Process.*, vol. 62, no. 6, Mar. 2014, pp. 1561–1575.

[14] M. Razaviyayn, G. Lyubeznik, and Z. Luo, "On the Degrees of Freedom Achievable through Interference Alignment in a MIMO Interference Channel," *IEEE Trans. Signal Process.*, vol. 60, no. 2, Feb. 2012, pp. 812–821.

[15] R. Yao et al., "Space Alignment Based on Regularized Inversion Precoding in Cognitive Transmission," *Radio Eng.*, vol. 24, no. 3, Sept. 2015, pp. 824–829.

[16] L.S. Cardoso et al., "Orthogonal LTE Two-Tier Cellular Networks," *IEEE Int. Conf. Commun.*, Kyoto, Japan, June 5–9, 2011, pp. 1–5.

[17] R. Yao et al., "Cooperative Precoding for Cognitive Transmission in Two-Tier Networks," preprint, submitted to *IEEE Trans. Commun.*, May 2015.

[18] R. Yao et al., "Cooperative Capacity-Achieving Precoding Design for Multi-user VFDM Transmission," *IEEE Global Conf. Signal Inf. Process.*, Atlanta, GA, USA, Dec. 3–5, 2014, pp. 1296–1300.

[19] T. Hasegawa, "Efficient Multi-antenna Expansion Method for Vandermonde-Subspace Frequency Division Multiplexing for 5G New Waveform," *IEEE Int. Symp. Pers., Indoor Mobile Radio Commun.*, Hong Kong, China, Aug. 30–Sept. 2, 2015, pp. 867–871.

[20] A. Goldsmith, "*Wireless Communications*," Cambridge, UK: Cambridge University Press, 2005, p. 363.

[21] J.L. Yu and D.Y. Hong, "A Novel Subspace Channel Estimation with Fast Convergence for ZP-OFDM Systems," *IEEE Trans. Wireless Commun.*, vol. 10, no. 10, Oct. 2011, pp. 3168–3173.

[22] H. Sung, S.R. Lee, and I. Lee, "Generalized Channel Inversion Methods for Multiuser MIMO Systems," *IEEE Trans. Commun.*, vol. 57, no. 11, Nov. 2009, pp. 3489–3499.

[23] D. Tse and P. Viswanath, "*Fundamentals of Wireless Communication*," Cambridge, UK: Cambridge University Press, 2005, pp. 332–382.

[24] D.A. Harville, "*Matrix Algebra from a Statistician's Perspective*," Berlin, German: Springer, 1997, p. 416.

[25] H.S. Witsenhausen, "A Determinant Maximization Problem Occurring in the Theory of Data Communication," *SIAM J. Appl. Math.*, vol. 29, no. 3, Nov. 1975, pp. 515–522.

[26] Y.S. Cho et al., "*MIMO-OFDM Wireless Communication with MATLAB*," Singapore: John Wiley & Sons, 2010, pp. 139–142.

[27] Q.H. Spencer, A.L. Swindlehurst, and M. Haardt, "Zero-Forcing Methods for Downlink Spatial Multiplexing in Multiuser MIMO Channels," *IEEE Trans. Signal Process.*, vol. 52, no. 2, Feb. 2004, pp. 461–471.

Rugui Yao received his BS, MS, and PhD degrees in telecommunications and information systems from the School of Electronics and Information (SEI), Northwestern Polytechnical University (NPU), Xi'an, China, in 2002, 2005, and 2007, respectively. From 2007 to 2009, he worked as a post-doctoral fellow at NPU. Since 2009, he has been with SEI, NPU, where he is now an associate professor. In 2013, he joined ITP Lab at Georgia Tech, Atlanta, USA, as a visiting scholar. He has worked in the areas of cognitive radio networks, channel coding, OFDM transmission, and spread-spectrum systems.

Juan Xu received her BS, MS, and PhD degrees in computer science and technology from the School of Computer, Northwestern Polytechnical University, Xi'an, China, in 2002, 2005, and 2011, respectively. Since 2011, she has been with the School of Electronic and Control Engineering, Chang'an University, Xi'an, China, where she is now an associate professor. Her main research interests are channel coding, OFDM transmission, and spread-spectrum systems.

Geng Li received his BS and MS degrees in telecommunications and information systems from the School of Electronics and Information, Northwestern Polytechnical University, Xi'an, China, in 2012 and 2015, respectively. His research interests include wireless communications and anti-jamming techniques.

Ling Wang received his BS, MS, and PhD degrees in electronic engineering from Xidian University, Xi'an, China, in 1999, 2002, and 2004, respectively. From 2004 to 2007, he worked for Corporate Technology of Siemens, Beijing, China, as a research scientist. In 2007, he joined the School of Electronics and Information, Northwestern Polytechnical University, Xi'an, China, as an associate professor, where he became a professor in 2012. His main research interests include smart antennas, wide-band transmission, adaptive anti-jamming for satellite communications, and satellite navigation.